

Thermally induced anchoring of a zinc-carboxyphenylporphyrin on rutile TiO₂ (110)

Res Jöhr, Antoine Hinaut, Rémy Pawlak, Łukasz Zajac, Piotr Olszowski, Bartosz Such, Thilo Glatzel, Jun Zhang, Matthias Muntwiler, Jesse J. Bergkamp, Luis-Manuel Mateo, Silvio Decurtins, Shi-Xia Liu, and Ernst Meyer

Citation: *The Journal of Chemical Physics* **146**, 184704 (2017);

View online: <https://doi.org/10.1063/1.4982936>

View Table of Contents: <http://aip.scitation.org/toc/jcp/146/18>

Published by the [American Institute of Physics](#)

Articles you may be interested in

[Characterization of individual molecular adsorption geometries by atomic force microscopy: Cu-TCPP on rutile TiO₂ \(110\)](#)

The Journal of Chemical Physics **143**, 094202 (2015); 10.1063/1.4929608

[Conformational adaptation and manipulation of manganese tetra\(4-pyridyl\)porphyrin molecules on Cu\(111\)](#)

The Journal of Chemical Physics **146**, 092316 (2017); 10.1063/1.4974313

[Forces from periodic charging of adsorbed molecules](#)

The Journal of Chemical Physics **146**, 092327 (2017); 10.1063/1.4975607

[Ordered heteromolecular overlayers formed by metal phthalocyanines and porphyrins on rutile titanium dioxide surface studied at room temperature](#)

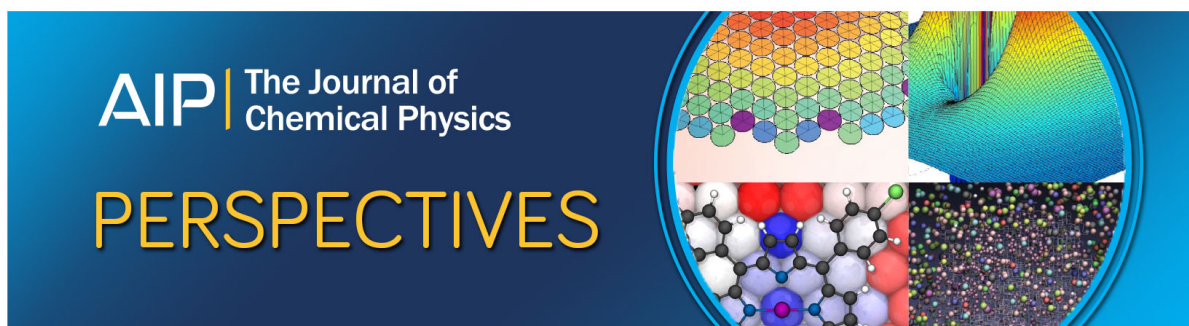
The Journal of Chemical Physics **143**, 224702 (2015); 10.1063/1.4936658

[Chemical bond imaging using higher eigenmodes of tuning fork sensors in atomic force microscopy](#)

Applied Physics Letters **110**, 183102 (2017); 10.1063/1.4982801

[Dibromobianthryl ordering and polymerization on Ag\(100\)](#)

The Journal of Chemical Physics **146**, 184701 (2017); 10.1063/1.4982939



Thermally induced anchoring of a zinc-carboxyphenylporphyrin on rutile TiO₂ (110)

Res Jöhr,¹ Antoine Hinaut,¹ Rémy Pawlak,¹ Łukasz Zajac,² Piotr Olszowski,² Bartosz Such,² Thilo Glatzel,¹ Jun Zhang,³ Matthias Muntwiler,³ Jesse J. Bergkamp,⁴ Luis-Manuel Mateo,⁴ Silvio Decurtins,⁴ Shi-Xia Liu,⁴ and Ernst Meyer^{1,a)}

¹Department of Physics, University of Basel, Klingelbergstrasse 82, 4056 Basel, Switzerland

²Physics Department, Jagiellonian University, Ul. Prof. St. Łojasiewicza 11, 30-348 Krakow, Poland

³Paul Scherrer Institute, 5232 Villigen, Switzerland

⁴Department of Chemistry and Biochemistry, University of Bern, Freiestrasse 3, 3012 Bern, Switzerland

(Received 20 February 2017; accepted 10 April 2017; published online 11 May 2017)

Functionalization of surfaces has become of high interest for a wealth of applications such as sensors, hybrid photovoltaics, catalysis, and molecular electronics. Thereby molecule-surface interactions are of crucial importance for the understanding of interface properties. An especially relevant point is the anchoring of molecules to surfaces. In this work, we analyze this process for a zinc-porphyrin equipped with carboxylic acid anchoring groups on rutile TiO₂ (110) using scanning probe microscopy. After evaporation, the porphyrins are not covalently bound to the surface. Upon annealing, the carboxylic acid anchors undergo deprotonation and bind to surface titanium atoms. The formation of covalent bonds is evident from the changed stability of the molecule on the surface as well as the adsorption configuration. Annealed porphyrins are rotated by 45° and adopt another adsorption site. The influence of binding on electronic coupling with the surface is investigated using photoelectron spectroscopy. The observed shifts of Zn 2p and N 1s levels to higher binding energies indicate charging of the porphyrin core, which is accompanied by a deformation of the macrocycle due to a strong interaction with the surface. *Published by AIP Publishing.* [<http://dx.doi.org/10.1063/1.4982936>]

I. INTRODUCTION

The deposition of well-designed molecules to a surface enables controlled assembly of functional nano-architectures by chemical reactions of adsorbates among each other or with the surface.^{1–3} Therefore, surface functionalization with organic molecules facilitates bottom-up fabrication of customized materials. The resulting surface and interface properties seem unlimited, considering the different substrates and the huge amount of organic molecules available. The general idea of this approach is to alter the surface properties by the addition of functional molecules. However, surface functionalization also gives rise to new interesting hybrid organic-inorganic interfaces. Tailoring of the interface allows one to exploit and benefit from processes such as charge transfer and electronic coupling of molecular orbitals with the surface. Both are crucial for molecular electronics, catalysis, and photovoltaics.^{4–9} The properties of the molecule and their interaction with the surface can be tuned with functional chemical groups. Especially important are the so-called anchoring groups that show a strong adsorption to the substrate and are used for the immobilization of molecules on surfaces, which is essential for stable interfaces.^{10–13} The use of multiple anchors further enables one to steer the orientation of the molecule on the surface. This directly affects the electronic coupling of the molecule with the surface and thereby the molecular properties as well.¹¹

Porphyrin sensitized titanium dioxide has been one of the most intensively studied systems for surface functionalization due to its suitability for photovoltaics, catalysis, and sensor applications.^{7,14–16} Porphyrins are ideal model sensitizers for systematic studies because they can be customized by modifying the substituents on the meso positions of the macrocycle as well as their ability to chelate a wide variety of transition metals within the macrocyclic core.^{17–20} This has been used to a great extent to control their optical and electronic properties as well as their self-assembly structures on metals.^{1,2} Furthermore, they are chemically and thermally robust and can be deposited by thermal evaporation. Consequently, many different porphyrin-titania systems have been investigated under ultra-high vacuum (UHV) conditions by scanning probe techniques and photoelectron spectroscopy (PES).^{21–31} Carboxylic acid substituents have often been used for immobilization of porphyrins on TiO₂.^{14,19} However, for relatively large porphyrins, which have been evaporated to the surface, it is often not clear if the anchoring group really undergoes reaction with the surface.^{21,23–25}

Here we show that the chemical linking of carboxylic anchors can be induced by thermal activation. We demonstrate this for zinc(II) 5,15-bis(4-carboxyphenyl)-10,20-diphenylporphyrin (ZnDCPP, see Figure 1(a)) evaporated onto rutile TiO₂ (110). The structure of the surface is depicted in Figure 1(c). Low temperature scanning tunneling microscopy (LT-STM) measurements reveal that freshly deposited porphyrins are all in one configuration, which is supposed to be stabilized by the interaction of the anchors to the substrate

^{a)}Electronic mail: ernst.meyer@unibas.ch

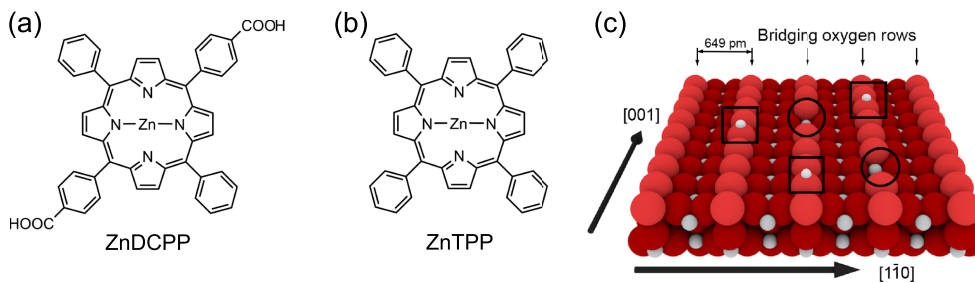


FIG. 1. Molecular structures of (a) zinc(II) 5,15-bis(4-carboxyphenyl)-10,20-diphenylporphyrin (ZnDCPP) and (b) zinc(II) 5,10,15,20-tetraphenylporphyrin (ZnTPP). (c) A model of the rutile TiO_2 (110) surface with defects. The size of the atoms is drawn corresponding to their ionic radii, which highlights the rows along the [001] direction. Oxygen vacancies and hydrogen adatoms are marked with circles and squares, respectively.

bridging oxygen atoms.²¹ Subsequent annealing results in a change of the porphyrin configuration on the surface, which we interpret as the deprotonation and subsequent carboxylate binding of the anchor with surface titanium atoms. The stability of the molecules against tip induced displacements observed by non-contact atomic force microscopy (nc-AFM) at room temperature further underlines that the annealed molecules are immobilized by covalent bonds with the surface. This is corroborated by LT-STM experiments with zinc(II) 5,10,15,20-tetraphenylporphyrin (ZnTPP, see Figure 1(b)), which has no anchor group and remains unchanged after annealing. These scanning probe studies are complemented by photoelectron spectroscopy, in order to investigate the influence of the adsorption mode on the coupling with the substrate.

II. METHODS

Nc-AFM experiments were made with a UHV room temperature nc-AFM developed at the University of Basel.³² The base pressure was lower than $2 \cdot 10^{-11}$ mbar. Measurements were done using silicon cantilevers (PPP-NCL, Nanosensors). Prior to measurement, cantilevers were prepared by thermal annealing (100 °C, 1 h) and Ar^+ sputtering (680 eV, 90 s). Topography images were recorded using the resonance frequency shift as feedback signal.³³ During the measurement, the averaged contact potential difference (CPD) between tip and sample was compensated by applying a constant bias voltage to the sample.

Scanning tunneling microscopy was performed on a low temperature STM from Omicron Nanotechnology GmbH at the Photoemission and Atomic Resolution Laboratory (PEARL) at the Paul Scherrer Institute (PSI) in Villigen CH. Images were taken using the constant current mode with the bias voltage applied to the tungsten tip.

Photoelectron spectroscopy (PES) measurements were done at the PEARL beamline of the Swiss Light Source (SLS).³⁴ The sample preparation was checked prior to PES experiments using STM. After this, the sample was transferred to the PES chamber under UHV. The spectra were fitted with Unifit using Voigt functions, which are a convolution of the natural line shape, given by a Lorentz profile and the instrument response function described by a Gaussian peak. The peak width of a certain core level was fixed to be the same for all the fits of a particular core level.

The samples were freshly prepared on site for each measurement. Rutile TiO_2 (110) single crystals (MaTeck GmbH) were prepared by repeated cycles of Ar^+ sputtering (1000 eV, 10 min) and subsequent annealing (800 °C, 15 min). The sample temperature was monitored using an infrared pyrometer measuring the temperature of the resistively heated silicon upon which the sample was mounted. The porphyrins used in this study were prepared by published protocols.^{35–37} Zinc(II) 5,10,15,20-tetraphenylporphyrin (ZnTPP) and zinc(II) 5,15-bis(4-carboxyphenyl)-10,20-diphenylporphyrin (ZnDCPP) were evaporated from a molecular evaporator at 275 °C and 350 °C, respectively. For the AFM investigation, the molecules were deposited to the substrate at room temperature. For STM and PES measurements, porphyrins were evaporated to the substrate held at 77 K. For both preparation setups, the annealing was done by resistive heating of the sample plate. The temperature of the sample was controlled with a thermocouple mounted close to the sample (Uni Basel) or estimated from calibrated dissipated power-temperature data (PSI).

It is noted that freshly prepared surfaces contain a small number of defects, which are either bridging oxygen vacancies or hydrogen adatoms (see Figure 1(c)). For this study, the defect density after preparation was estimated by STM to be about 5%. This means that 5% of the bridging oxygen sites contained a defect. The number of defects typically increases with time due to adsorption of, e.g., residual water molecules.³⁸ In order to avoid the interaction of the porphyrins with defects, they were always evaporated to freshly prepared surfaces.

III. RESULTS AND DISCUSSION

A. Adsorption modes of ZnDCPP and ZnTPP

Figure 2(a) shows a constant current LT-STM image of ZnDCPP evaporated to the surface held at 77 K. The STM images show that the porphyrins adsorb in one single molecular orientation, which is aligned along the [001]-rows of the surface. The STM topography images were acquired with positive sample bias and represent empty states of the substrate. Therefore, the oxygen rows in Figure 2(a), which are marked with dashed lines, appear lower in height than the titanium atoms.³⁹ This type of the rows can also be assigned by considering that the defects such as hydrogen adatoms or

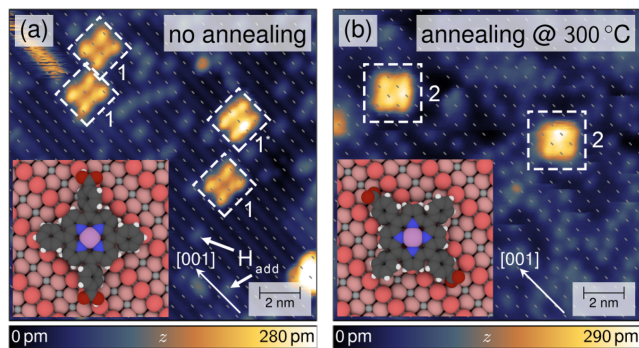


FIG. 2. Constant current STM images of ZnDCPP on rutile TiO_2 (110): (a) After evaporation to the cold rutile TiO_2 (110) surface. The molecule denoted by 1* indicates a porphyrin with brighter contrast, which is interacting with a defect below ($V_{\text{sample}} = 1.5$ V, $I_t = 15$ pA). (b) After annealing to 300 °C ($V_{\text{sample}} = 2.0$ V, $I_t = 10$ pA). The common STM contrast of the substrate is inverted in this image due to a tip change. Oxygen rows are indicated with dashed lines in each case and the inset shows proposed models for the two adsorption configurations.

oxygen vacancies only appear on the bridging oxygen rows (see Figure 1(c)). In our case, there are mainly hydrogen adatoms (H_{add}), which appear as small dot-like protrusions. From this, we deduce that the zinc porphyrin cores are situated on the oxygen atom rows. The axis of the carboxyphenyl groups has a 45° angle with respect to the [001]-rows (see Figure 2(a)). This orientation allows for the stabilization of the molecules by direct interaction, presumably hydrogen bonds, of the anchors with the bridging oxygen atoms. A proposed binding configuration is shown in the inset of Figure 2(a). For further reference, we will denote this adsorption mode as configuration 1. As indicated in this figure, we note that not all porphyrins show the same contrast, which is due to interaction with subjacent defects.^{30,40}

In order to promote the formation of covalent bonds between carboxylic acids and the surface titanium atoms, the sample was heated to 300 °C for 30 min. Figure 2(b) shows the constant current STM image of the obtained surface. The molecules are again in one single orientation but are rotated by 45°. We refer to this orientation as configuration 2 and note that the surface shows more hydrogen adsorbates after annealing. A portion of the hydrogen atoms is suspected to originate from the deprotonation of the carboxylic acids. Other

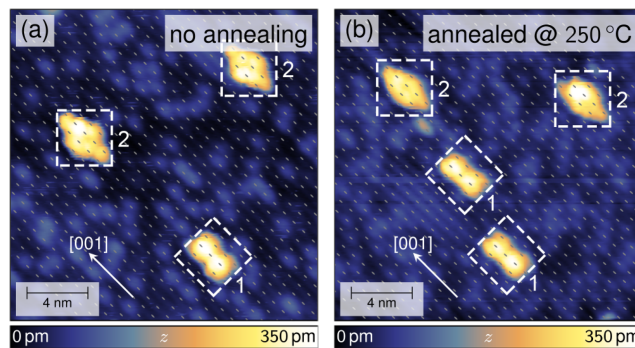


FIG. 3. Constant current STM images of ZnTPP on rutile TiO_2 (110): (a) after evaporation to the cold substrate ($V_{\text{sample}} = 1.8$ V, $I_t = 20$ pA) and (b) after 30 min annealing to 250 °C ($V_{\text{sample}} = 1.8$ V, $I_t = 10$ pA).

hydrogen atoms originate from residual water molecules in the preparation chamber that adsorbs dissociatively to oxygen vacancies during the annealing in the preparation chamber.³⁸ Despite the adsorbates, the molecules are still lying flat on the surface. We note that Figure 2(b) reveals an inverted substrate imaging contrast. The hydrogen adsorbates are now on the bright rows. It is assumed that this contrast inversion is due to a tip change, which happened during *in situ* tip preparation on the surface. Nonetheless, our assignment of the surface atoms is still unambiguous since we also observed the normal STM contrast on the same sample but with lower resolution on the molecules. A similar observation on bare rutile (110) has been made, for example, by Diebold and co-workers.³⁹ Considering the contrast inversion, we find that the center of the porphyrins is now shifted to a titanium row. In this configuration, the carboxyl groups can easily anchor to surface titanium atoms. A suggestive model of the adsorption configuration is depicted in the inset of Figure 2(b).

In order to justify the above interpretation, we repeated the same experiment for ZnTPP, which is a structural control that bears no carboxylic acid anchors capable of binding to the surface. After evaporation, the ZnTPP is found in two distinct adsorption modes as shown in Figure 3(a) and denoted therein as 1 and 2. The ZnTPP adopts the same two orientations and binding sites as previously described for ZnDCPP, the molecules, however, look slightly elongated along the

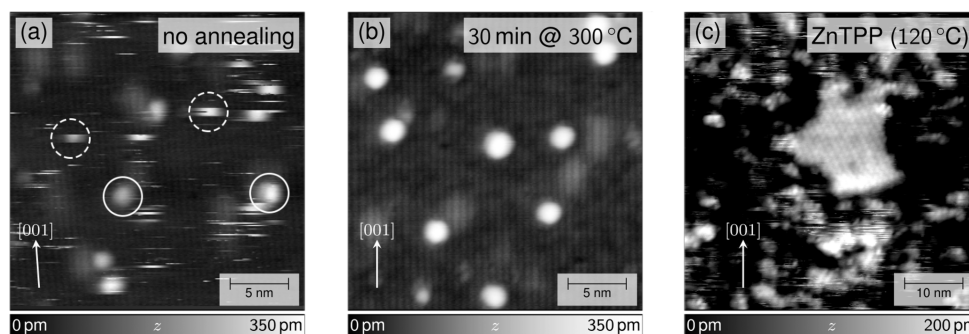


FIG. 4. Nc-AFM topography images of ZnDCPP on rutile TiO_2 (110): (a) After deposition to the sample held at room temperature. Some of the moving and stable molecules are marked with dashed and solid circles, respectively. (b) After 30 min annealing at 300 °C (PPP-NCL, $f_1 = 156.7$ kHz, $A_1 = 10$ nm, $\Delta f_1 = -4$ Hz, $Q_1 = 29.9$ k). (c) Nc-AFM topography of a ZnTPP island after mild annealing to 120 °C (PPP-NCL, $f_2 = 978.5$ kHz, $A_2 = 400$ pm, $\Delta f_2 = -30$ Hz, $Q_2 = 13.5$ k). The z-range was reduced to increase the contrast on the island.

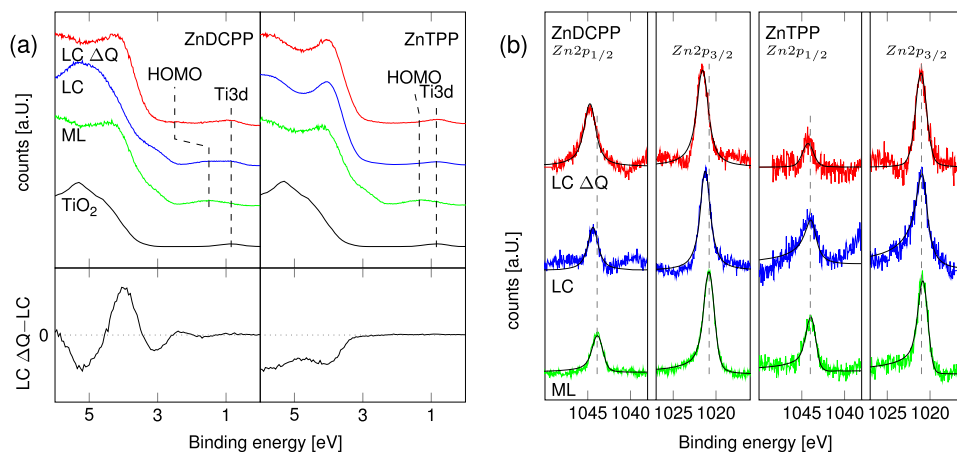


FIG. 5. PES spectra of ZnDCPP and ZnTPP on rutile TiO_2 (110) for submonolayer coverage after deposition (LC), after annealing (LC Δ Q), and multilayer (ML) coverage: (a) Valence band spectra obtained with a photon energy of $h\nu = 65$ eV. (b) PES of Zn2p obtained with a photon energy of $h\nu = 1253$ eV. The dashed lines indicate the position of the highest occupied molecular orbitals. The graphs at the bottom show the changes upon annealing.

[001]-direction. This is an imaging artefact resulting from an asymmetric tip, which is likely due to *in situ* tip modification on the surface. Again we observe inverted imaging contrast on the substrate. Nevertheless, the two orientations can be clearly distinguished. From a set of 50 molecules, we estimate the ratio of the two configurations to be approximately 1:1. After annealing to 250°C , the STM images still reveal these two orientations (Figure 3(b)). The ratio of the two configurations slightly changed to 4:3 in favor of the configuration 2 after annealing. However, this finding is most probably due to evaporation of the less interacting configuration 1 as will be justified later by the PES measurements. The STM results indicate that only the ZnDCPP rotates due to annealing, which is clear evidence that the carboxylic anchors are involved in the rotation and that they react with the surface.

B. Stability of ZnDCPP configurations

Nc-AFM measurements were directly made after evaporation of ZnDCPP to the freshly prepared rutile TiO_2 (110) surface. The topography image in Figure 4(a) shows many noise lines, which represent displacements of molecules that are caused by interaction with the scanning tip.^{41,42} Only few stable ZnDCPPs are observed and appear as bright dots with a diameter of about 2 nm. They are mainly found on the terraces. Hardly any ZnDCPP adsorbs on the step edges thus implying that these porphyrins have limited intrinsic mobility and stay close to their landing sites. Our observations allow us to categorize two types of ZnDCPPs. One that is weakly bound and can be manipulated with the tip and another one that is stable. Annealing to 300°C for 30 min improves the scan stability. The streak lines are no longer present meaning that all ZnDCPPs are now in the stable configuration and linked to the surface (see Figure 4(b)). Manipulation of the porphyrins could not be achieved anymore. Further decreasing the tip-sample distance in order to enable the manipulation resulted in tip crashes. For comparison, nc-AFM topography images obtained for ZnTPP are generally fuzzy and there is no improvement of the scan condition upon annealing, suggesting that the annealing does not anchor the ZnTPP. In contrary, the formation of islands was observed for higher coverages, which indicates that the mobility of ZnTPP is increased (see Figure 4(c)). Thus it is evident that the diffusion barrier of ZnDCPP is already increased by the

carboxylic acid anchors. In fact, the initial adsorption configuration of ZnDCPP after deposition is supposed to be stabilized by hydrogen bonds. Hence it becomes obvious that there must be an even stronger type of molecule-surface interaction to facilitate the immobilization. Therefore, these AFM results support the hypothesis of covalent bond formation under annealing.

C. Molecular energy levels

The binding of molecules to the substrate can affect the energy levels of the adsorbate and thus change its properties such as light absorption properties. The resulting electronic structure at the interface can further influence charge transfer between the molecule and the substrate, which is a desired process in hybrid photovoltaics. In order to correlate the adsorption configuration with the molecular properties, PES measurements were conducted on the non-annealed submonolayer (LC, for low coverage), the annealed submonolayer (LC Δ Q), and on freshly deposited multilayers (MLs) of porphyrins. The multilayer measurements were performed in order to get the reference data of the porphyrins without surface interaction.

The valence band spectra are shown in Figure 5(a). In order to compensate for molecule induced work function shifts, spectra of porphyrin covered surfaces have been shifted to align the known Ti 3d defect state of the substrate, which is at 0.87 eV.^{43,44} The highest occupied molecular orbitals (HOMOs) are marked in the spectra and the extracted binding energies (BEs) are given in Table I. The HOMO is particularly important for the optical transitions in the molecule. Shifts of

TABLE I. Binding energies of Zn 2p, N 1s levels, and the highest occupied molecular orbitals from PES.

		HOMO (eV)	Zn 2p _{1/2} (eV)	Zn 2p _{3/2} (eV)	N 1s (eV)	
ZnDCPP	ML	1.50	1043.9	1020.8	397.5	...
	LC	1.51	1044.3	1021.2	397.6	...
	LC Δ Q	2.42	1044.8	1021.6	397.7	398.5
ZnTPP	ML	1.29	1044.0	1020.9	397.4	...
	LC	1.37	1044.1	1021.0	397.5	...
	LC Δ Q	1.41	1044.2	1021.0	397.5	398.3

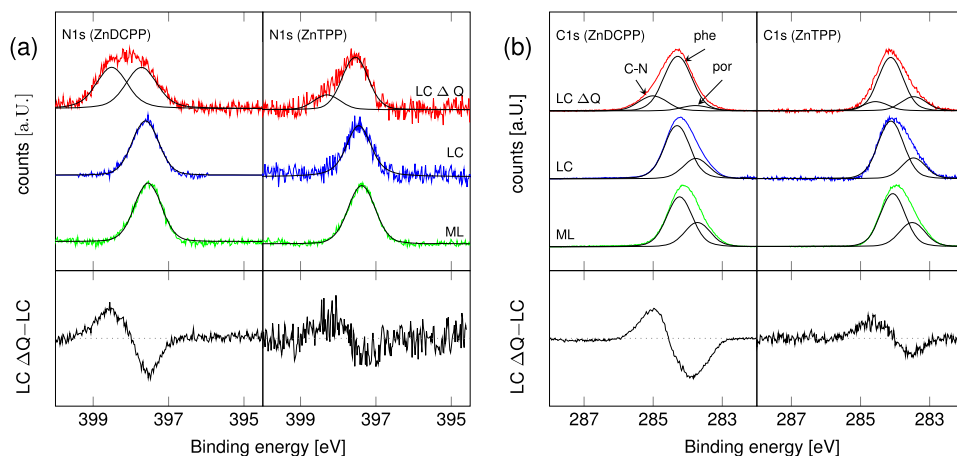


FIG. 6. PES spectra of ZnDCPP and ZnTPP on rutile TiO_2 (110) for sub-monolayer coverage after deposition (LC), after annealing (LC Δ Q), and multilayer (ML) coverage: (a) N 1s spectra obtained with a photon energy of $h\nu = 500$ eV. (b) C 1s spectra obtained with a photon energy of $h\nu = 340$ eV. The bottom graph shows the relative difference between the just deposited molecules and after annealing.

the HOMO are commonly linked to changes of the absorption wavelength. The HOMO of the multilayer is at binding energies of 1.50 eV and 1.29 eV for ZnDCPP and ZnTPP, respectively. In the LC spectra, these levels are hardly shifted and overlapped partially with the Ti 3d defect state of the titania surface. The HOMO of ZnDCPP shifts to higher binding energy upon annealing as indicated in the difference spectrum of Figure 5(a). The positive shift of the HOMO after annealing is attributed to positive charging of the molecule.³⁰ For ZnTPP, the HOMO intensity was rather low, making it hard to correctly identify the HOMO position. However, the comparison of the complete valence band spectra as well as the difference spectrum in Figure 5(a) suggested that there is no further shift after heating. The main change was a loss of ca. 20% in signal intensity that was caused by re-evaporation of the porphyrins. In contrast to the HOMOs, the LUMOs are not supposed to be significantly affected by the charging as was, for example, shown for CuTCPP.³⁰ They were thus not investigated in more detail.

The BE of the Zn 2p levels for the two porphyrins are given in Table I and the spectra are depicted in Figure 5(b). For both porphyrins, the Zn 2p peak of the low coverage is shifted to higher binding energy compared to the multilayer spectrum, as indicated by the dashed lines in Figure 5(b). This suggests partial charging due to coupling with the surface. For ZnDCPP, this effect amounts to 0.4 eV whereas it is 0.1 eV for ZnTPP. Since the Zn 2p peak is expected to shift to lower binding energy by about 1.0 eV in the case of demetalation, we conclude that the molecules keep their metal cores.²⁷ The position of the ZnDCPP Zn 2p peak is further shifted by about 0.4 eV after annealing, which is attributed to further charging of the core. This shift is not observed for ZnTPP.

Further information on the coupling of the porphyrin core with the substrate can be obtained from the spectra of the N 1s core level, which are depicted in Figure 6(a). The peaks of the N 1s for the ML and LC coverage of the porphyrins are at the same position and consist of a single component (see Table I). The spectra of the annealed porphyrins show a broadened or asymmetric peak for ZnDCPP or ZnTPP, respectively, which indicates the presence of two components. The energy difference between these two peaks is 0.8 eV. The LC Δ Q ZnDCPP N 1s spectrum can be fitted with two peaks of equal

amplitude. Since there is one dominant adsorption configuration, our results suggest that the nitrogen atoms of ZnDCPP are no longer indistinguishable after annealing. This could be an evidence for the distortion of the porphyrin macrocycle which might be due to stronger electrostatic interaction induced by the observed charging.

The ZnDCPP spectrum gives evidence that the second peak in the ZnTPP N 1s spectrum is related to the orientation of the molecules. However, the rotation alone does not suffice for explanation. From the STM experiments, it is known that both orientations are already present for the just deposited ZnTPP. Nevertheless, the second N 1s peak hardly shows up before annealing. Since the ratio of the two modes does hardly change during annealing, we conclude that the porphyrin has to be in the orientation 2 after evaporation and subsequently annealed in order to show a splitting of the N 1s core level. Thus the correct orientation of the porphyrin core is a prerequisite for the increased interaction with the substrate, which is thermally activated. Since the two orientations have different interaction strengths, we conclude that ZnTPP in configuration 1 is preferably re-evaporated during annealing, therefore, explaining the altered ratio of the two configurations. The shape of the C 1s spectra is in good agreement with these observations. The spectra of the LC porphyrins show an asymmetry and were fitted with two peaks (Figure 6(b)). One for the phenyl (phe) contributions and one for the carbons of the delocalized porphyrin core (por). After annealing there is another contribution at a BE of 285 eV, which is at the cost of the porphyrin core peak. This peak corresponds to C–N bonds and shows the same shift as the N 1s peak described before.

IV. CONCLUSION

In conclusion, we observed the anchoring process of ZnDCPP on rutile TiO_2 (110) by means of low temperature STM. The formation of covalent bonds to the surface was induced by annealing the evaporated porphyrins. The initially H-bond stabilized molecule underwent deprotonation and formed covalent bonds between the carboxylate anchors and surface titanium atoms. This process was accompanied by a 45° rotation of the ZnDCPP. The interpretation of this experiment was corroborated by the study of ZnTPP, which was

not able to form chemical bonds and showed no significant change upon annealing. Further evidence for the immobilization of ZnDCPP was given by nc-AFM at room temperature, where the stability against manipulation with the scanning tip was assessed. The coupling with the substrate was investigated using valence band spectroscopy and showed that charge transfer to the substrate was increased if the molecule was anchored by a carboxylate.

The described anchoring process is expected to be possible for other large carboxylic acid bearing molecules on rutile TiO₂ (110) as well. Thereby the efficiency of the surface reaction is presumably higher if the molecule is adapted to the surface topography. If the molecule does not match or cannot adapt to the surface, it might still react. In this case, molecules with more than one anchoring group might only bind with some of them.

ACKNOWLEDGMENTS

The authors thank Ali Sadeghi from the Shahid Beheshti University Theran for fruitful discussions. The Swiss National Science Foundation (SNF), the Swiss Nanoscience Institute (SNI), and the Joint Swiss-Polish Research Programme PSPB-085/2010 are acknowledged for financial support. We acknowledge the Paul Scherrer Institut, Villigen, Switzerland for provision of synchrotron radiation beamtime at beamline X03DA/PEARL of the SLS.

- ¹W. Auwärter, D. Écija, F. Klappenberger, and J. V. Barth, *Nat. Chem.* **7**, 105 (2015).
- ²J. V. Barth, *Annu. Rev. Phys. Chem.* **58**, 375 (2007).
- ³N. Kocic, X. Liu, S. Chen, S. Decurtins, O. Krejci, P. Jelinek, J. Repp, and S.-X. Liu, *J. Am. Chem. Soc.* **138**, 5585 (2016).
- ⁴M. Jurow, A. E. Schuckman, J. D. Batteas, and C. M. Drain, *Coord. Chem. Rev.* **254**, 2297 (2010).
- ⁵E. Leary, A. La Rosa, M. T. Gonzalez, G. Rubio-Bollinger, N. Agrait, and N. Martin, *Chem. Soc. Rev.* **44**, 920 (2015).
- ⁶B. O'Regan and M. Grätzel, *Nature* **353**, 737 (1991).
- ⁷R. Zhang, A. A. Elzatahry, S. S. Al-Deyab, and D. Zhao, *Nano Today* **7**, 344 (2012).
- ⁸R. Jöhr, L. Zajac, G. Günzburger, H. Hug, B. Such, M. Szymonski, E. Meyer, and T. Glatzel, *Hybrid Mater.* **2**, 17 (2015).
- ⁹A. Amacher, C. Yi, J. Yang, M. P. Bircher, Y. Fu, M. Cascella, M. Grätzel, S. Decurtins, and S.-X. Liu, *Chem. Commun.* **50**, 6540 (2014).
- ¹⁰F. Chen, X. Li, J. Hihath, Z. Huang, and N. Tao, *J. Am. Chem. Soc.* **128**, 15874 (2006).
- ¹¹P. Rahe, M. Kittelmann, J. L. Neff, M. Nimrich, M. Reichling, P. Maass, and A. Kühnle, *Adv. Mater.* **25**, 3948 (2013).
- ¹²L. Zhang and J. M. Cole, *ACS Appl. Mater. Interfaces* **7**, 3427 (2015).
- ¹³Y. Fu, S. Chen, A. Kuzume, A. Rudnev, C. Huang, V. Kaliginedi, M. Baghernejad, W. Hong, T. Wandlowski, S. Decurtins, and S.-X. Liu, *Nat. Commun.* **6**, 6403 (2015).
- ¹⁴A. Yella, H.-W. Lee, H. N. Tsao, C. Yi, A. K. Chandiran, M. Nazeeruddin, E. W.-G. Diau, C.-Y. Yeh, S. M. Zakeeruddin, and M. Grätzel, *Science* **334**, 629 (2011).
- ¹⁵J. Niu, B. Yao, Y. Chen, C. Peng, X. Yu, J. Zhang, and G. Bai, *Appl. Surf. Sci.* **271**, 39 (2013).
- ¹⁶A. A. Ismail and D. W. Bahnemann, *ChemSusChem* **3**, 1057 (2010).
- ¹⁷S. Ahmadi, M. N. Shariati, S. Yu, and M. Göthelid, *J. Chem. Phys.* **137**, 084705 (2012).
- ¹⁸J. Rochford, D. Chu, A. Hagfeldt, and E. Galoppini, *J. Am. Chem. Soc.* **129**, 4655 (2007).
- ¹⁹R. B. Ambre, G.-F. Chang, and C.-H. Hung, *Chem. Commun.* **50**, 725 (2014).
- ²⁰R. Ambre, K.-B. Chen, C.-F. Yao, L. Luo, E. W.-G. Diau, and C.-H. Hung, *J. Phys. Chem. C* **116**, 11907 (2012).
- ²¹R. Jöhr, A. Hinaut, R. Pawlak, A. Sadeghi, S. Saha, S. Goedecker, B. Such, M. Szymonski, E. Meyer, and T. Glatzel, *J. Chem. Phys.* **143**, 094202 (2015).
- ²²L. Zajac, P. Olszowski, S. Godlewski, B. Such, R. Jöhr, R. Pawlak, A. Hinaut, T. Glatzel, E. Meyer, and M. Szymonski, *J. Chem. Phys.* **143**, 224702 (2015).
- ²³L. Zajac, P. Olszowski, S. Godlewski, L. Bodek, B. Such, R. Jöhr, R. Pawlak, A. Hinaut, T. Glatzel, E. Meyer, and M. Szymonski, *Appl. Surf. Sci.* **379**, 277 (2016).
- ²⁴P. Olszowski, L. Zajac, S. Godlewski, B. Such, R. Jöhr, T. Glatzel, E. Meyer, and M. Szymonski, *J. Phys. Chem. C* **119**, 21561 (2015).
- ²⁵S. Godlewski and M. Szymonski, *Int. J. Mol. Sci.* **14**, 2946 (2013).
- ²⁶S. Rangan, S. Coh, R. A. Bartynski, K. P. Chitre, E. Galoppini, C. Jaye, and D. Fischer, *J. Phys. Chem. C* **116**, 23921 (2012).
- ²⁷A. Rienzo, L. C. Mayor, G. Magnano, C. J. Satterley, E. Ataman, J. Schnadt, K. Schulte, and J. N. O'Shea, *J. Chem. Phys.* **132**, 084703 (2010).
- ²⁸C. Wang, Q. Fan, S. Hu, H. Ju, X. Feng, Y. Han, H. Pan, J. Zhu, and J. M. Gottfried, *Chem. Commun.* **50**, 8291 (2014).
- ²⁹C. Wang, Q. Fan, Y. Han, J. I. Martinez, J. A. Martin-Gago, W. Wang, H. Ju, J. M. Gottfried, and J. Zhu, *Nanoscale* **8**, 1123 (2016).
- ³⁰R. Pawlak, A. Sadeghi, R. Jöhr, A. Hinaut, T. Meier, S. Kawai, L. Zajac, P. Olszowski, S. Godlewski, B. Such, T. Glatzel, S. Goedecker, M. Szymonski, and E. Meyer, *J. Phys. Chem. C* **121**, 3607 (2017).
- ³¹S. Rangan, C. Ruggieri, R. Bartynski, J. I. Martínez, F. Flores, and J. Ortega, *J. Phys. Chem. C* **120**, 4430 (2016).
- ³²L. Howald, E. Meyer, R. Lüthi, H. Haefke, R. Overney, H. Rudin, and H. Güntherodt, *Appl. Phys. Lett.* **63**, 117 (1993).
- ³³T. R. Albrecht, P. Grütter, D. Horne, and D. Rugar, *J. Appl. Phys.* **69**, 668 (1991).
- ³⁴M. Muntwiler, J. Zhang, R. Stania, F. Matsui, P. Oberta, U. Flechsig, L. Patthey, C. Quitmann, T. Glatzel, R. Widmer, E. Meyer, T. A. Jung, P. Aebi, R. Fasel, and T. Greber, *J. Synchrotron Radiat.* **24**, 354 (2017).
- ³⁵A. D. Adler, F. R. Longo, J. D. Finarelli, J. Goldmacher, J. Assour, and L. Korsakoff, *J. Org. Chem.* **32**, 476 (1967).
- ³⁶C. He, Q. He, C. Deng, L. Shi, D. Zhu, Y. Fu, H. Cao, and J. Cheng, *Chem. Commun.* **46**, 7536 (2010).
- ³⁷K. Lu, C. He, and W. Lin, *J. Am. Chem. Soc.* **136**, 16712 (2014).
- ³⁸O. Bikondoa, C. L. Pang, R. Ithnin, C. A. Muryn, H. Onishi, and G. Thornton, *Nat. Mater.* **5**, 189 (2006).
- ³⁹U. Diebold, J. Lehman, T. Mahmoud, M. Kuhn, G. Leonardelli, W. Hebenstreit, M. Schmid, and P. Varga, *Surf. Sci.* **411**, 137 (1998).
- ⁴⁰M. Lackinger, M. S. Janson, and W. Ho, *J. Chem. Phys.* **137**, 234707 (2012).
- ⁴¹M. Watkins, T. Trevethan, A. L. Shluger, and L. N. Kantorovich, *Phys. Rev. B* **76**, 245421 (2007).
- ⁴²B. Such, T. Trevethan, T. Glatzel, S. Kawai, L. Zimmerli, E. Meyer, A. L. Shluger, C. H. M. Amijs, P. de Mendoza, and A. M. Echavarren, *ACS Nano* **4**, 3429 (2010).
- ⁴³S. Wendt, P. T. Sprunger, E. Lira, G. K. H. Madsen, Z. Li, J. O. Hansen, J. Matthiesen, A. Blekinge-Rasmussen, E. Lægsgaard, B. Hammer, and F. Besenbacher, *Science* **320**, 1755 (2008).
- ⁴⁴A. G. Thomas, W. R. Flavell, A. K. Mallick, A. R. Kumarasinghe, D. Tsoutsou, N. Khan, C. Chatwin, S. Rayner, G. C. Smith, R. L. Stockbauer, S. Warren, T. K. Johal, S. Patel, D. Holland, A. Taleb, and F. Wiame, *Phys. Rev. B* **75**, 035105 (2007).